Journal of the Iranian Chemical Society (2022) 19:147–158
https://doi.org/10.1007/s13738-021-02294-w

ORIGINAL PAPER

Synthesis and applications of some new nitrogen-containing heterocyclic azo-disperse dyes bearing quinoline chromophore

Khalid Mahmoud Hassan[1,2] · **Shaban Abdel Sattar ElKhabiery**[3] · **Ghada Mahmoud ElHaddad**[4] · **Sameha Hassan Shokair**[4] · **Ibrahim ElTantawy ElSayed**[4]

Received: 17 December 2020 / Accepted: 25 May 2021 / Published online: 6 June 2021

Abstract

A set of five novel nitrogen-containing heterocyclic azo-disperse dyes **8 (a–d)** and **10** were synthesized by diazotization of 4-bisaminoquinolines **3**, followed by coupling either with rhodanine analogues **6** modified at C-5 position or α-naphthol **9**. The chemical structures of **8(a–d)** and **10** were proven by the FT-IR, NMR, and mass spectroscopic techniques. Moreover, utilization of these azo dyes in preparing pastes for printing polyester fabric by silk screen traditional printing was achieved. The color strength and fastness properties of the synthesized dyes were also examined and showed moderate-to-excellent resistance to washing, rubbing, and perspiration, as well as fastness to sublimation and light. In addition, the targeted printed samples were screened for their in vitro antibacterial activity against both Gram-positive and Gram-negative bacterial species. The azo compound **8a** showed the best antibacterial activity against *S. aureus* with inhibition zone of 23 mm which is higher than the reference drug Ampicillin (21 mm).

Keywords Amino quinolines · Azo-disperse dyes · Diazotization · Printing polyester · Antibacterial activity

Introduction

Azo-disperse dyes are one of the most common and efficient classes of synthetic industrial dyes. Synthetic azo compounds [1, 2] now became widely spread in handling much applications in both medical field and textile industries [3, 4]. In recent years, the development of heterocyclic azo-disperse dyes compounds containing nitrogen atom was vital structural units in dyeing textiles and in medicinal chemistry. These derivatives proved to be important scaffolds in both textile printing and biological chemistry [5]. They had significant biological activity as anticancer [6, 7], antifungal [8], antibacterial [1, 2], antioxidant [2], antitumor [8], anti-inflammatory [9] antimalarial [8] and other industrial applications in pharmaceutical [10, 11], cosmetic [12], photography [13], paints [13, 14], and textiles [15]. Most dyes are classified according to their chemical structures [16] or application methods. Chemical classification of these dyes is very important as it depends upon the functional groups present in a molecule [17]. Because of the wide applications of azo compounds, it was interesting to study the synthesis of new azo compounds, which derived from amino quinoline motif. In addition, quinoline- and rhodanine-containing azo dyes have numerous properties encompassing inherent color deepening effect as a key feature of the quinoline and rhodanine rings [18–22]. Based on the above-mentioned facts, we aim to construct azo-disperse dyes derived from quinoline and/or rhodanine and study their biological and industrial applications as antibacterial and dyes on textile fibers, respectively.

✉ Khalid Mahmoud Hassan
drkhalidhassan73@gmail.com;
drkhalidhassan73@el-eng.menofia.edu.eg

✉ Ibrahim ElTantawy ElSayed
ibrahimtantawy@yahoo.co.uk

[1] Electrochemistry Research Laboratory, Physics and Mathematics Engineering Department, Faculty of Electronic Engineering, Menoufia University, Menouf 23952, Egypt

[2] Applied Sciences Department, Higher College of Technology, University of Technology and Applied Sciences, Al-Khuwair, PO Box 74, 133 Muscat, Oman

[3] Dyeing, Printing and Textile Auxiliaries Department, Textile Research Division, National Research Centre, 33 El Bohouth street, Dokki, P.O.12622, Giza, Egypt

[4] Chemistry Department, Faculty of Science, Menoufia University, Shebin El-Kom, Egypt

Experimental section

Instruments and methods

All ^{1}H- and ^{13}C-NMR spectra were recorded on a JEOL ECA500 FT NMR spectrometer at 500 MHz and 100 MHz at El-Mansoura and Zagazig University Central Laboratory, Egypt in which dimethyl sulfoxide (DMSO-d6) was used as solvent. Chemical shifts were expressed in δ ppm relative to the position respective to the solvent. Fourier transform infrared (FT-IR) spectra were recorded using Thermo Fisher Nicolet IS10, Spectral Analyses Unit, Faculty of Science, Mansoura University, Egypt. Electron impact ionization mass spectra (EI-MS) were obtained on a Thermos Scientific Trace 1310 Mass Spectrometry et al.-Azhar University, Egypt. UV/vis absorption spectra for azo compounds were measured by a Hunter Lab Ultra Scan PRO spectrophotometer. The in vitro antibacterial screening was carried out at Micro Analytical Center, Cairo University, Egypt. Melting points (m.p) were measured and recorded by Stuart scientific melting point apparatus and were uncorrected. All synthetized products were detected by thin-layer chromatography (TLC) on kiesel gel F254 precoated plates (Merck). Compounds **3a**, **6a** and **6b** were prepared according to the reported methods [23–27].

Chemicals and reagents

4,7-Dichloroquinoline (99%), 1,4-phenylenediamine (99%), 4,4′-methylenedianiline (97%), rhodanine (97%), and allyl rhodanine were obtained from Sigma Aldrich. α-Naphthol (99%), salicylaldehyde (99%), triethylamine (Et_3N) (99%), ethanol (EtOH) (99%), glacial acetic acid (Gal. AcOH, 99.7%), dichloromethane (DCM, 99.8%), hydrochloric acid (HCl, 35.4%), sodium nitrite ($NaNO_2$, 98%), sodium carbonate (Na_2CO_3, 98%), sodium dihydrogen phosphate (98.0%), and sodium lignosulfonate (anionic dispersing agent, powder) (99.5%) were bought from LOBA Chemie. Sodium acetate (AcONa, 99%) was obtained from East-Chem. Thickener (commercial synthetic thickener) acrylate copolymers and Lyprint (sodium salt of nitrobenzene sulfonic acid) were supplied from BASF Company. Polyester (150 g/m^2) were supplied by Egyptian and developing Co., Cairo, Egypt. Daico thick 1600, a synthetic thickener for azo-disperse silk screen-printing, was supplied by Daico company. All chemicals and reagents were used without any further purification.

General synthetic method for rhodanine derivatives [6]

A mixture of salicylaldehyde **4** (0.42 mL, 4 mmol) and rhodanine **5a** (0.95 g, 4.0 mmol) or allyl rhodanine **5b** (0.69 g, 4.0 mmol) was dissolved in Gal. AcOH acid in presence of AcONa (0.33 g, 12.0 mmol) and then refluxed for 4 h. The reaction completion was monitored by TLC using DCM and EtOH mixture (5:1) as eluent. The reaction mixture was cooled to room temperature and poured dropwise into crushed ice. The precipitated product was filtered off, washed by deionized water, and then dried to afford **6**.

2-(2-Hydroxybenzylidene)-5-thioxodihy drothiophen-3(2H)-one [6b] Yellowish powder; yield (0.81 g, 81%); m.p (148–150 ºC); FT-IR (cm^{-1}) = 3228 (OH), 3050 (=CH), 2924 (-CH_2-), 1680 (C=O), 1588 (C=C), 1205 (C = S). ^{1}H-NMR (DMSO-d_6, ppm): δ = 4.63 (m, 2H, C$\underline{H}_2$=CH), 5.20 (m, 2H, CH=C$\underline{H}_2$), 5.83 (m, 1H, C$\underline{H}$ = CH_2), 6.95–7.73 (m, 4H, CH_{Ar}), 8.07 (s, 1H, C$\underline{H}$=C), 10.74 (br. s, 1H, OH). EI-MS (*m/z*) ($C_{13}H_{14}NO_2S_2$): calcd, 280; found molecular ion peak 279 $[M-1]^+$.

General synthetic method for azoquinoline derivatives [8 (a–d) and 10]

A mixture of the appropriate aryl amine **3a** (0.27 g, 1.0 mmol) or **3b** (0.36 g, 1.0 mmol) and concentrated (conc. HCl) acid (2.0 mL, 34%) in 25.0-mL glass beaker was stirred using a magnetic stirrer and subsequently cooled to 0–5 °C in an ice bath. An aqueous solution of $NaNO_2$ (0.069 g, 1.0 mmol) in water (3.0 mL) is then added slowly. The produced diazonium salt **7** was stirred for an extra 30 min at 0–5 °C. In a separate glass beaker, cooled rhodanine analogues **6** modified at C-5 position or α-naphthol **9** (1.0 mmol) was dissolved in EtOH (5.0 mL) and cooled to 0–5 °C, and then, Na_2CO_3 (1.0 g, 10.0 mmol) was added. The produced mixture was vigorously stirred in the ice bath at 0–5 °C, while the cold diazonium salt solution was added portion-wise. After stirring for an extra two hours, the crude product was filtered off under vacuum, washed several times with distilled water (5.0 mL), recrystallized from EtOH, and air-dried to afford the azo compounds **8(a–d)** and **10** in excellent yields.

5-((4-((7-Chloroquinolin-4-yl) amino) phenyl) diazenyl)-2-hydroxybenzylidene)-2-thioxothiazolidin-4-one [8a] Yellow powder; yield (0.80 g, 80%); m.p (178–180 °C); FT-IR (cm^{-1})=3661–3353 (OH), 3462 (NH), 3039 (=CH), 1675

(C=O), 1568 (C=C), 1526 (CN), 1450 (N=N), 1221 (C=S). ^{1}H-NMR (DMSO-d_6): $\delta = 6.90$- 7.95 (*m*, 9H, CH_{Ar}), 8.14 (*s*, 1H, HC=C), 8.45–8.62 (*m*, 3H, CH_{Ar}), 9.30 (br. s, 1H, NH), 9.30, 9.51 (br. s, 2H, 2NH), 10.41 (*s*,1H, OH). ^{13}C-NMR (DMSO-d_6): $\delta = 101.38$, 116.11, 117.75, 119.81, 121.72, 122.86, 123.96, 124.83, 125.76, 126.94, 127.97, 128.97, 131.63, 132.05, 135.02, 137.18, 143.14, 147.69, 149.95, 151.91, 157.34, 173.31, 197.89.EI-MS (*m/z*) ($C_{25}H_{16}ClN_5O_2S_2$): calcd, 517; found molecular ion peak 517 [M^+].

5-((4-((7-Chloroquinolin-4-yl)amino)phenyl)diazenyl)-2-hydroxybenzylidene)-2-thioxothiazolidin-4-one [8b] Dark yellow powder; yield (0.78 g, 78%); m.p (140–142 °C); FT-IR (cm^{-1}) = 3706–3118 (OH), 3419 (NH), 3058 (=CH), 2924 (-CH), 1701 (C=O), 1571 (C=C), 1527 (C=N), 1450 (N=N), 1209 (C=S). ^{1}H-NMR (DMSO-d_6,ppm): $\delta = 4.63$ (*d*, $J = 5.0$ Hz, 2H, –CH_2), 5.18 (*m*, 2H, HC=CH_2), 5.82 (*m*, 1H,CH=CH_2), 7.33–7.91 (*m*, 9H, CH_{Ar}), 8.14 (*s*, 1H, CH=C), 8.34–8.45 (*m*, 3H, CH_{Ar}), 9.20 (br. s, 1H, NH), 10.80 (br. s, 1H, OH). EI-MS (*m/z*) ($C_{28}H_{20}ClN_5O_2S_2$): calcd, 557; found molecular ion peak 556 [M-1]$^+$.

5-((4-(4-((6-Chloronaphthalen-1-yl) amino) benzyl) phenyl) diazenyl)-2-hydroxybenzylidene)-2-thioxothiazolidin-4-one [8c] Yellow powder; yield (0.83 g, 83%); m.p (170–172 °C); FT-IR (cm^{-1}) = 3721–3147 (OH), 3411 (NH), 3030 (=CH), 2920 (CH_2), 1702 (C=O), 1573 (C=C), 1512 (C=N), 1448 (N=N), 1212 (C=S). ^{1}H-NMR (DMSO-d_6): $\delta = 4.06$ (s, 2H, CH_2), 6.85–7.82 (*m*, 13H, CH_{Ar}), 8.14 (*s*, 1H, CH=C), 8.41- 8.45 (*m*, 3H, CH_{Ar}), 9.23 (br. s, 2H, 2NH), 10.40 (*s*, 1H, OH). ^{13}C-NMR (DMSO-d_6): $\delta = 101.36$, 116.14, 117.89, 119.77, 120.86, 122.63, 123.29, 123.92, 124.96, 125.26, 127.98, 128.85, 129.78, 129.90, 131.70, 134.71, 137.39, 137.48, 137.88, 144.48, 145.20, 148.00, 149.19, 150.73, 151.93, 158.57,160.10, 162.35, 198.79. EI-MS (*m/z*) ($C_{32}H_{22}ClN_5O_2S_2$): calcd, 607; found molecular ion peak 607 [M^+].

5-((4-(4-((6-Chloronaphthalen-1-yl) amino) benzyl) phenyl) diazenyl)-2-hydroxybenzylidene)-2-thioxothiazolidin-4-one [8d] Dark yellow powder; yield (0.65 g, 65%); m.p (136–138 °C); FT-IR (cm^{-1}) = 3706–3118 (OH), 3388 (NH), 3031 (=CH), 2920 (CH), 1684 (C=O), 1579 (C = C), 1511 (C=N), 1453 (N=N), 1206 (C=S). ^{1}H-NMR (DMSO-d_6): $\delta = 3.98$ (s, 2H, CH_2), 4.63 (s, 2H, –CH_2), 5.15 (m, 2H, HC=CH_2), 5.82 (m, 1H, CH=CH_2), 6.85–7.88 (*m*, 13H, CH_{Ar}), 8.13 (*s*, 1H, CH=C), 8.34 (*m*, 3H, CH_{Ar}), 9.20 (br. s, 1H, NH), 10.78 (*s*, 1H, OH). ^{13}C-NMR (DMSO-d_6):$\delta = 46.00$, 101.40, 116.11, 116.32, 117.77, 117.98, 119.22, 119.92, 120.03, 120.64, 123.29, 124.56, 124.93, 126.80, 127.95, 128.91, 129.68, 129.73, 129.83, 130.32, 131.61, 133.17, 134.34, 137.15, 137.73, 148.48, 148.85, 151.09, 151.90, 158.54, 166.79, 199.52. EI-MS (*m/z*) ($C_{35}H_{26}ClN_5O_2S_2$): calcd, 648; found molecular ion peak 648 [M^+].

4-((4-(4-((6-Chloronaphthalen-1-yl) amino) benzyl) phenyl) diazenyl) naphthalen-1-ol [10] Dark brown powder; yield (0.71 g, 71%); m.p (130–132 °C); FT-IR (cm^{-1}) = 3662–3279 (OH), 3241(NH), 2923 (–CH), 1596 (C=C), 1533 (C=N), 1450 (N=N). ^{1}H-NMR (DMSO-d_6): $\delta = 4.16$ (s, 2H, CH_2), 7.00–7.90 (*m*, 16H, CH_{Ar}), 8.20 (*m*, 2H, CH_{Ar}), 8.88 (*m*, 1H, CH_{Ar}), 9.30 (*s*, 1H, NH), 11.12 (br. s, 1H, OH). EI-MS (*m/z*) ($C_{32}H_{23}ClN_4O$): calcd, 514; found molecular ion peak 514 [M^+].

Textile printing

Preparation of printing paste

Each printing paste was prepared using the proportions shown in Table 1.

The aforementioned printing paste was applied to polyester fabrics according to conventional screen-printing method [28]. Prints fixation was carried out by drying at room temperature followed by thermo-fixation for 4 min at 180 °C. The prepared prints were rinsed in hot water, cold water and soaped with 2.0 g/L nonionic detergent at 60 °C for 30 min, respectively.

Determination of antibacterial activity

The target polyester-printed azo dyes were further used individually to analyze its antibacterial activity against human pathogens, Gram-positive bacteria such as *Staphylococcus aureus* ATCC6538, *Bacillus subtilis* ATCC6633, and *Streptococcus faecalis* and Gram-negative bacteria for instance *Escherichia coli* ATCC8739, *Pseudomonas aeruginosa* ATCC9022, and *Neisseria gonorrhoeae.*

Each bacterial strain was inoculated in to L. B. broth media and incubated at 35 ± 2 °C for 24 h, then, 100 µL of each bacterial strain (1 × 108 CFU/mL) was seeded onto Muller Hinton agar media under aseptic condition and poured into petri dishes. 1.0 cm^2 of polyester-printed azo dyes were aseptically prepared and put onto the surface of

Table 1 The components of the printing paste

Dye	4.0 g
Thickener	75.0 g
Lyprint	3.0 g
Sodium dihydrogen phosphate	5.0 g
Sodium lignosulfonate	1.0 g
Water	12.0 g
Total	100.0 g

seeded Muller Hinton agar plate and kept in the refrigerator for 2 h before incubation at 35 ± 2 °C for 24 h. After incubation, the plates were examined and the diameters of inhibition zones (mm) were recorded around the fabric samples. The antibacterial behaviors of loaded polyester fabrics were analyzed after four washing cycles for the following treatments; (A) standard disk of ampicillin (antibacterial agent) as positive control, (B) starting material which coded as **1** (4,7-dichloro quinoline), (C) untreated polyester fabrics as negative control, and (D) polyester fabrics loaded with azo dyes **8(a–d)** and **10** [29].

The protocol method as following, 100 µL of the tested bacteria were grown in 10 mL of fresh media until they reached a count of approximately 108 cells/mL for bacteria [30, 31]. 100 µL of bacterial suspension was spread onto the agar plates corresponding to the broth in which they were maintained. Isolated colonies of each organism that might be playing a pathogenic role should be selected from primary agar plates and tested for susceptibility by disk diffusion method [32]. Plates inoculated with Gram-positive and Gram-negative bacteria were incubated at 35–37 °C for (24–48 h) and yeast as *Candida albicans* incubated at 30 °C for (24–48 h). The diameters of the inhibition zones were measured in millimeters [29]. Standard disks of Ampicillin (antibacterial agent) served as positive controls for antibacterial activity and filter disks impregnated with 10 µL of solvent (deionized water, chloroform, DMSO) were used as a negative control. Blank paper disks (Schleicher & Schuell, Spain) with a diameter of 8 mm were impregnated 10 µL of tested concentration of the stock solutions. When a filter paper disk impregnated with a tested chemical is placed on agar, the chemical will diffuse from the disk into the agar. This diffusion will place the chemical in the agar only around the disk. The solubility of the chemical and its molecular size will determine the size of the area of chemical infiltration around the disk. If an organism is placed on the agar, it will not grow in the area around the disk if it is susceptible to the chemical. This area of no growth around the disk is known as a "Zone of inhibition" or " Clear zone." For the disk diffusion, the zone diameters were measured with slipping calipers of the National Committee for Clinical Laboratory Standards [30, 31]. Agar-based methods such as Etest and disk diffusion can be good alternatives because they are simpler and faster than broth-based methods [33].

Results and discussion

Chemistry

In this study, we probed the synthesis, textile printing, and antibacterial evaluation of newly developed heterocyclic azo-disperse dyes. The synthetic approaches for quinoline-rhodanine or quinoline-α-naphthol conjugates are outlined in the schemes below. The starting 4-bisaminoquinolines **3** were obtained in good yields according to the reaction of 4,7-dichloroquinoline **1** with equimolar ratio of 1,4-phenylene diamine **2a** or 4,4′-methylenedianiline **2b** dissolved in EtOH in presence of Et_3N as a base under reflux for (14 -18 h) as shown in Scheme 1.

The plausible mechanism for the formation of **3** is depicted in Scheme 1. The nucleophilic aromatic substitution (S_{NAr}) of the amine nitrogen to the chloride ion at position C-4 is activated by the quinoline ring nitrogen via negative mesomeric effect through the formation of a resonance-stabilized anion **A**. This will assist the nucleophilic displacement of the chloride at C-4 position by amines nitrogen followed by its abstraction with the aid of Et_3N base to form triethylamine hydrochloride salt (Et_3N. HCl). The new C–N bond formation via charged intermediates **A** and **B** eventually lead to the formation of the expected 4-bisaminoquinolines **3** as depicted in Scheme 1.

Furthermore, structure-bearing quinoline-rhodanine conjugates were obtained via Knoevenagel condensation reaction [34, 35]of salicylaldehyde **4** with equimolar ratio of rhodanine analogues **5** in presence of AcONa/Gal.AcOH acid mixture as the catalyst. The reaction medium afforded phenolic-rhodanine congers **6** in good yields as depicted in Scheme 2.

The structure of compound **6b** was elucidated by FT-IR, ^{1}H-NMR and mass spectral analysis. The FT-IR spectra showed a characteristic OH broadband at 3228 cm^{-1}. While the > C=O and > C=S groups exhibited characteristic bands at 1680 and 1205 cm^{-1}, respectively. ^{1}H-NMR indicated doublet at 4.63 ppm which corresponds to $–CH_2$-aliphatic, the multiplet appeared at 5.20 ppm corresponding to terminal olefinic protons ($CH=C\underline{H}_2$), the multiplet appeared at 5.83 ppm relating to internal olefinic proton $C\underline{H}=CH_2$, the singlet appeared at 8.07 ppm is related to exocyclic bond $C\underline{H}=C$, and broad singlet appeared at 10.74 ppm for OH phenolic proton. The mass spectral analysis showed the expected molecular ion peaks, which confirmed the chemical structure.

The plausible mechanism for the formation of **6** through Knoevenagel condensation reaction was given in the following Scheme 2. This C–C bond formation reaction involved deprotonation of hydrogen from the active methylene group in rhodanine ring in **5** by the aid of AcONa as a base to afford the anionic intermediate **A** in situ. The subsequent nucleophilic addition of **A** to the electrophilic carbon atom of the formyl group in salicylaldehyde **4** yielded the intermediate **B**. Further, protonation of **B** with AcOH ease the dehydration with expelled of water to form the **6** in excellent yields as depicted in Scheme 2.

Having the starting key components **3** and **6** in hand, the formation of azo dyes **8 (a–d)** and **10** was achieved in

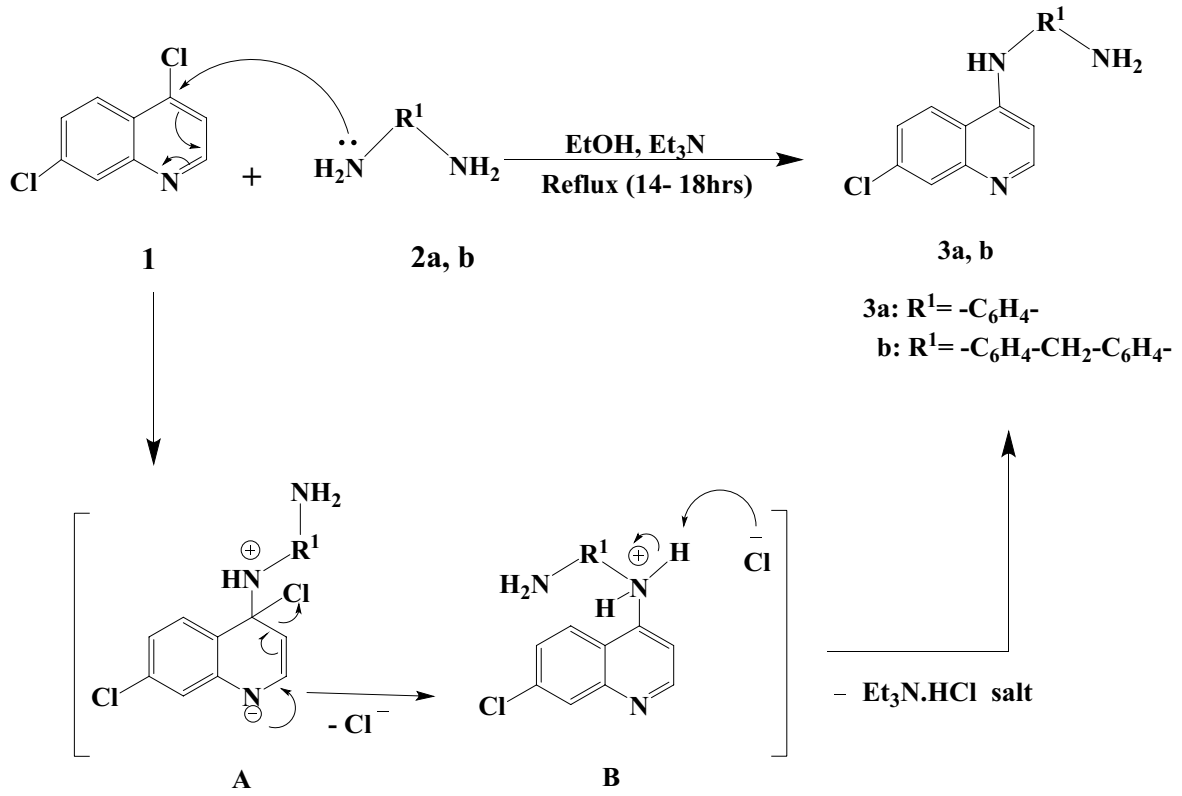

Scheme 1 Synthesis of 4-(bis-amino) quinolines **3**

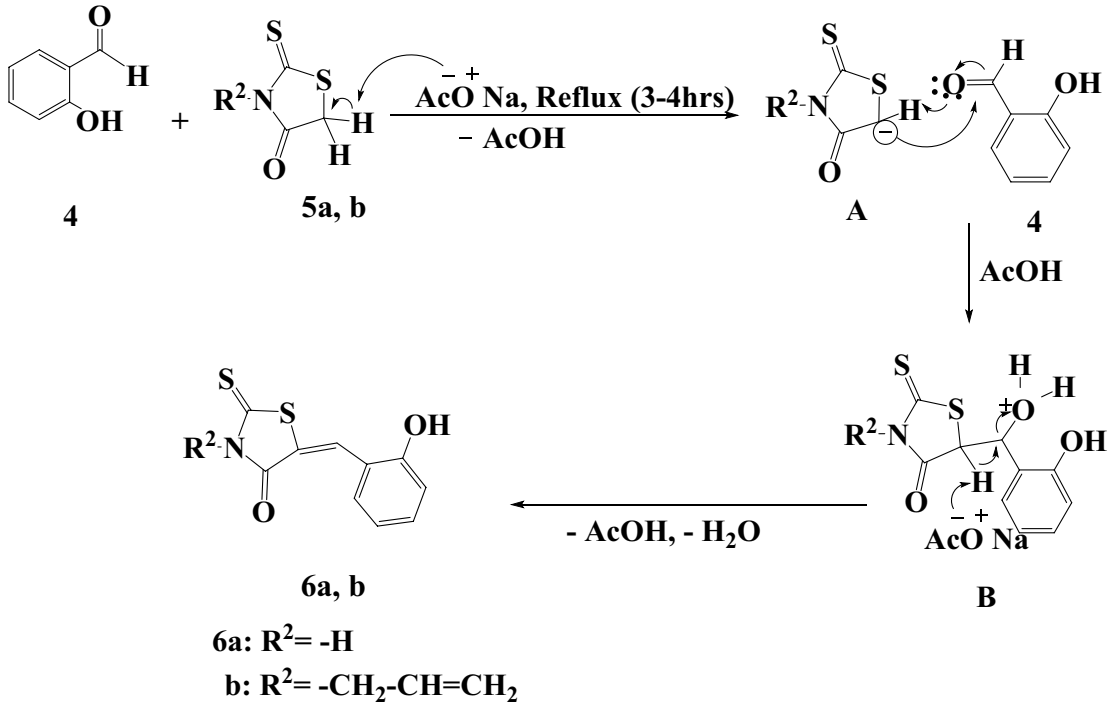

Scheme 2 Synthesis of congers **6** by Knoevenagel condensation reaction

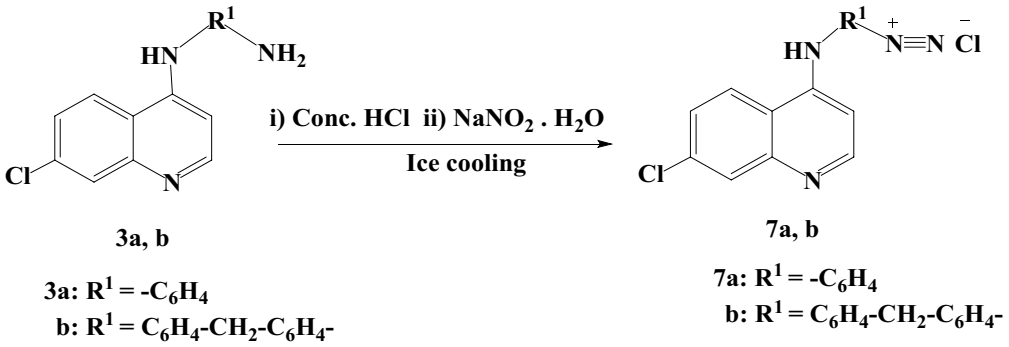

Scheme 3 Synthesis of the diazonium salts **7**

two-step reactions. The first step included the diazotization of bisaminoquinolines **3** with conc. HCl and $NaNO_2$ solution under ice cooling to afford the corresponding non-isolable reactive intermediate, quinoline diazonium chloride **7** as given in Scheme 3.

The second step included the coupling of the diazonium salt **7** (electrophile) with electron-rich component (nucleophile) such as phenolic derivatives **6** and **9.** This reaction was performed via an electrophilic aromatic substitution mechanism. The hydroxyl group directs the quinoline

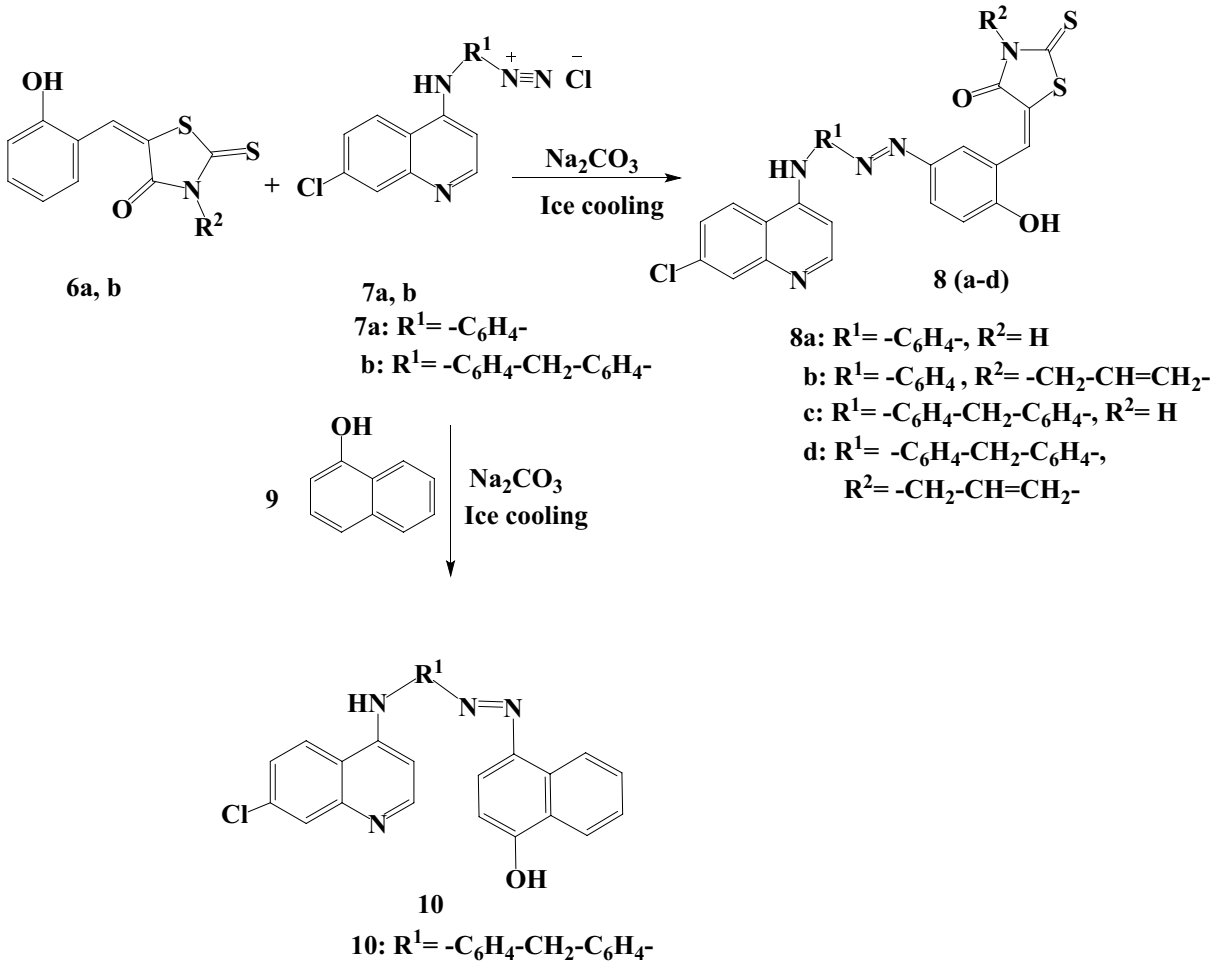

Scheme 4 Synthesis of azoquinoline derivatives of **8(a–d)** and 1**0**

diazonium ion to the para site of OH group in **6** and **9** under basic condition to afford the required azo-dye compounds **8 (a–d)** and **10** in excellent yields as depicted in Scheme 4.

The structure of compounds **8 (a–d)** and **10** was characterized by FT-IR, ^{1}H, ^{13}C-NMR and mass spectral analysis. The FT-IR spectra showed characteristic NH broadbands at 3462, 3419, 3411, 3388 cm^{-1} for **8a, b, c** and **d**, respectively. The OH group for **8 a–d** exhibited a characteristic broadband ranging from 3118 to 3721 cm^{-1}. Furthermore, > C=O group for **8 a–d** showed absorption band ranging from 1701- 1684 cm^{-1}. Moreover, the azo (–N=N–) group for **8 a–d** showed a characteristic band ranging from 1450 to 1426 cm^{-1}. ^{1}H-NMR indicated singlet at 4.06 and 3.98 ppm assigning to the aliphatic protons of (–C$\underline{H}_2$) for **8 c** and **d**. Moreover, the allylic methylene proton (–C$\underline{H}_2$) of **8 b** appeared at 4.63 ppm (J = 5.0 Hz), while the multiplet appeared at 5.15 and 5.18 ppm corresponding to the terminal olefinic proton (–CH=C$\underline{H}_2$) of the allyl group in **8 d** and **b**, respectively**.** In addition, the multiplet appeared at 5.82 ppm corresponding to the internal olefinic proton (–C$\underline{H}$ = CH_2) for both **8 b** and **d**. Furthermore, singlet appeared ranging from 7.88 to 8.14 ppm for (–C$\underline{H}$=C) exocyclic double bond which attached to rhodanine ring for **8 a**–**d**. In addition, two broad NH singlet appeared at 9.30 and 9.51 ppm for **8a**. The azo compounds **8 b–d** showed a broad singlet at 9.20, 9.23 and 9.20 ppm, respectively, corresponding to the NH group. On the other hand, the phenolic OH proton for **8 a–d** displayed a broad singlet ranging from 10.40 to 10.78 ppm. The ^{13}C-NMR (DMSO-d_6) of **8 a, c** and **d** showed signals at 166.79, 173.31, and 162.35 ppm for the carbon atom of > C=O group, and signals at 197.89, 198.79, and 194.52 ppm for the carbon atom of > C=S group, respectively.

The FT-IR spectrum for **10** showed broad OH absorption band ranging from 3662 to 3279 cm^{-1}, while exhibited a broad absorption band at 3241 cm^{-1} for the NH group. The absorption peaks appeared at 2923 and 1410 cm^{-1} corresponding to the aliphatic (–CH_2) and azo groups, respectively. ^{1}H-NMR spectrum for **10** showed NH and OH broad singlet at 9.30 ppm and 11.12 ppm, respectively. The mass spectral analysis for all products **8 (a–d)** and **10** showed the expected molecular ion peaks which confirmed the chemical structures.

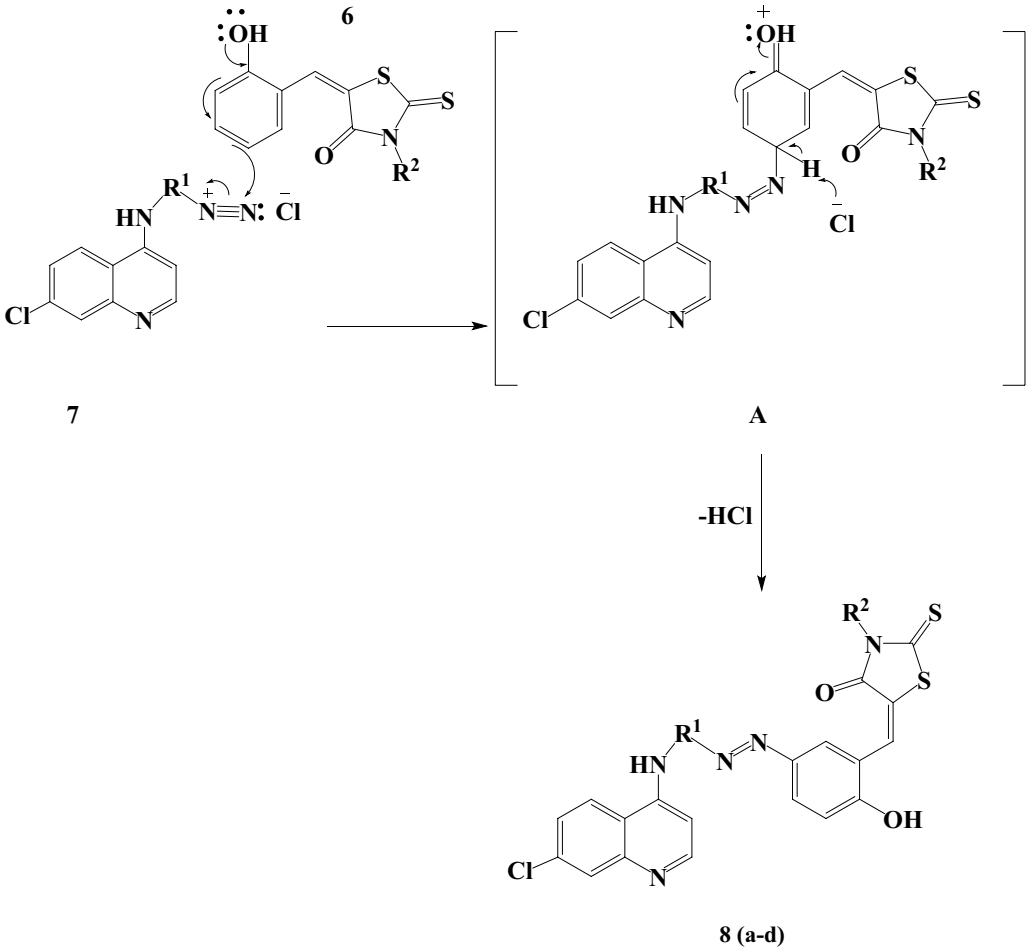

Scheme 5 Suggested mechanism of azoquinoline derivatives **8 (a–d)**

Scheme 6 Suggested mechanism of azoquinoline derivative **10**

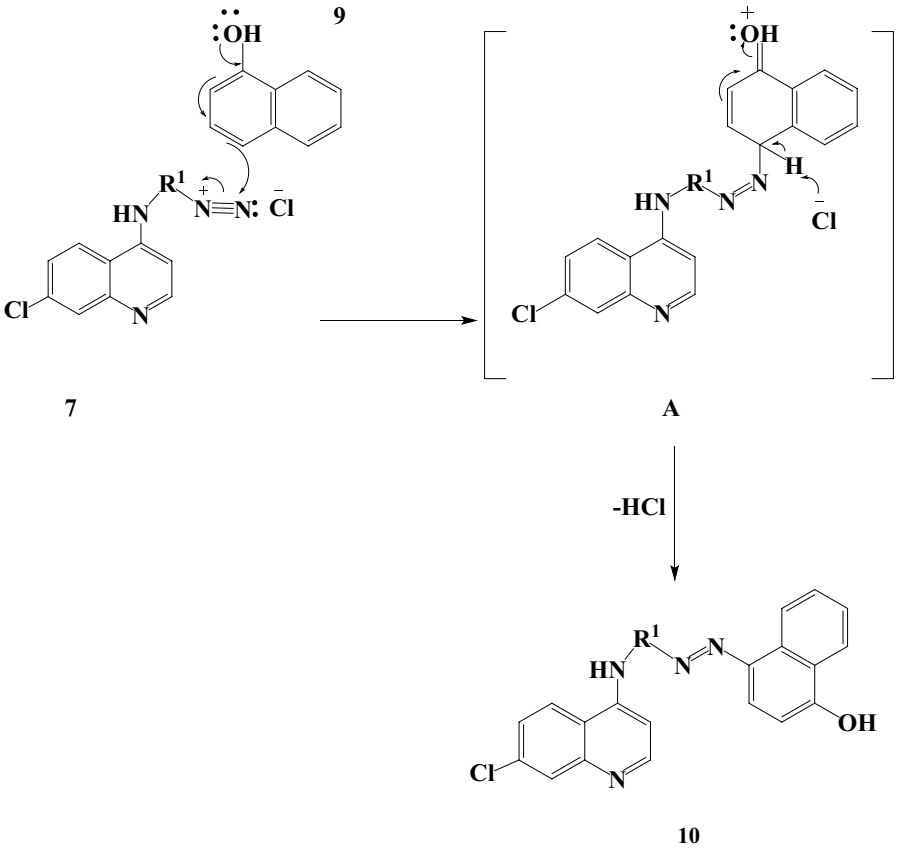

The proposed mechanism for the azo-dye formation is given in Schemes 5 and 6. The first step involved the formation of resonance-stabilized carbanion of phenol-rhodanine congers **6** and α-naphthol **9**. The second step included nucleophilic phenol-rhodanine or nucleophilic naphthol-quinoline congers generation, then attacks the electrophilic diazonium nitrogen in **7** to form the rhodanine-quinoline or quinoline naphthalic azo dyes **8 (a–d)** and **10** as depicted in Scheme 5 and Scheme 6.

Color strength measurements (K/S) and analyses

Color measurements

The colorimetric strength data of the printed polyester fabric samples were measured by light reflectance technique using a Hunter Lab Ultra Scan PRO spectrophotometer. The color strength was expressed as (*K/S* value) using the following Kubelka–Munk Eq. 1.

$$K/S = \frac{(1-R)^2}{2R} \tag{1}$$

where R is a decimal fraction of the reflection of the dyed fabric, K is an absorption coefficient, and S is a scattering coefficient.

The K/S values were calculated from the reflectance values at the corresponding wavelength for each dye. As estimated from our experiments, the k/s for the prepared dyes; **8 a**, **b**, **c**, **d**, and **10** was measured at their corresponding wavelengths; 410, 425, 415, 412, and 435 nm, respectively. The obtained values represent the depth of dyeing which are proportional to the amount of colorant present in the dyed fabrics [36]. Table 2 shows color strength value (16.88) of azo compound **10** is higher than **8 (a–d)**, due to higher absorption of azo compound **10** (435 nm) than **8(a–d)**. This due to the high conjugation of **10**, the absorption peak wavelengths shifted toward the long wavelength region and the absorption peaks were larger than other dyes **8(a–d)**. The lightness (L*) of azo compound **10** (36.56) is lower than **8 (a–d)**. As the lower in lightness (L*), the deeper in the color on dyed fabric [37]. The chroma (saturation) (c*) and hue angle (h°) are calculated by using following equations [38, 39]:

$$c* = \sqrt{(a*)2 + (b*)2} \tag{2}$$

$$h = \tan^{-1}\left(\frac{a*}{b*}\right) \tag{3}$$

The color hues of the dyes **8 (a–d)** and **10** on the polyester fabric were shifted in the reddish—yellowish direction due

Table 2 Color assessment of the printed azo-disperse dyes samples

Dye	Color shade	Absorption [λ_{max} (nm)]	K/S	L*	a*	b*	C*	h
8 a	Yellow	410	12.14	56.14	15.14	33.14	35.32	65.18
8 b	Yellow	425	13.66	54.18	16.12	44.61	44.78	69.88
8 c	Yellow	415	12.88	59.44	17.58	40.88	39.23	69.14
8 d	Yellow	412	13.79	55.14	16.12	35.68	38.14	65.99
10	Brown	435	16.88	36.56	26.15	19.22	32.78	35.81

Lightness (L*), degree of redness (+ve) and greenness (ve) (a*), degree of yellowness (+ve) and blueness (-ve) (b*), chroma (C*), hue (h) and color strength (K/S)

to the positive values of a* and b*, respectively. Dye **10** produced higher color strength than dyes **8a–d**. This is due to the high conjugation of the naphthol coupler of dye **10** comparing with the rhodanine couplers in dyes **8a–d**.

Fastness properties

The fastness properties of the printed samples were measured to washing, perspiration, rubbing, light, and sublimation according to the standard ISO methods [40–44].

Washing fastness The color fastness to washing was measured according to the method ISO 105-C06 B2S [40]. Wash fastness is measured the resistance of dyed fibers to retain color when they are washed by detergents and soaps. The change in color of the dyed samples and the staining of the adjacent fabric is detected according to the standard grey scale as (1 = poor, 2 = moderate, 3 = good, 4 = very good, 5 = excellent). The polyester fabric printed with dyes **8d** and **10** showed very good-to-excellent results (4–5) than other printed dyes **8a**, **b**, and **c** which showed moderate-to-excellent results rating (2–5) as shown in Table 3. This due to the larger size of **8d**, it will be entrapped inside the interpolymer chain space of a poly ester fiber and increasing of hydrophobic nature by increasing aromatic rings of these dyes [45, 46]. The stability of dye **10** toward washing may be attributed to the good penetration and affinity of the dye **10** to the fiber structure which prevents the dye molecule from transferring to the fiber surface [47].

Perspiration fastness The color fastness to perspiration (acid and alkaline) was determined according to the method ISO 105-E04 [42]. It refers to the ability not to fade and not to stain when the dyed fabric is perspired. It is measured in accordance with the standard grey scale rating from 1 to 5 as (1) is poor and (5) is excellent. The polyester fabric printed with dyes **8d** showed very good-to-excellent results (4–5) than other printed dyes **8a**, **b**, **c**, and **10** which indicated moderate-to-excellent results rating (2–5) (Table 3). The higher the molecular weight of the dye, the lower rate of dye removal according to the influence of perspiration solution [48].

Rubbing fastness The color fastness to rubbing (wet and dry) was detected according to method ISO 105X12 [41]. It determines the degree of color transfer from the surface of the dyed fabric to another adjacent undyed fabric surface by rubbing. It was measured according to the standard gray scale which is rated between (1–5). The grade (1) is poor and (5) is excellent. The polyester fabric printed with dye **10** indicated very good-to-excellent results (4–5) in wet and dry fiber. While the printed dyes **8(a–d)** appeared moderate-to-very good results rating (2–4) (Table 3). Also, due to the high diffusion of dye **10** molecule into the fiber than other dyes **8 (a–d)** [49, 50].

Light fastness The color fastness to light was evaluated according to method ISO 105-B02 [44]. It measures the duration and the degree to which printed dyes resist fad-

Table 3 Fastness properties of the polyester fabric printed with dyes **8 (a–d) and 10**

Sample	Light fastness	Washing fastness[a]		Rubbing		Perspiration fastness[a]	
		St	Alt	Wet	Dry	St	Alt
8a	6	3–4	3–4	2–3	3–4	3–4	4–5
8b	5	3–4	4–5	4	2–3	3–4	3–4
8c	6	4–5	2–3	3–4	4–5	2–3	2–3
8d	6	4–5	4–5	3–4	4	4–5	4
10	7	4–5	4–5	4–5	4–5	3–4	4–5

[a]Alt. is an alteration in color and St. is a staining on cotton

ing because of constant light exposure. It was determined in accordance with the standard blue scale (1–8) as (1) is very poor and (8) is excellent. The printed dye **10** showed excellent result (7), while printed dyes **8(a–d)** showed good-to-very good results (5–6) as given in Table 3. The high results of **10** and **8 (a–d)** light due to the presence of electron withdrawing group (Cl) which increase brightness [51] in quinoline moiety of all dyes. The higher fastness to light of printed dye **10** than **8 (–d)** could be attribute to the huge electron-donating groups in **8(a–d)** which reduce the brightness properties [51].

Sublimation fastness The color fastness to sublimation was estimated according to method ISO 105P01 [43]. It determines the ability of the printed dyes resistance toward high temperature and pressure. It was measured using a fixometer at180 and 210^0C according to the standard grey scale (1–5) which (1 = poor, 5 = excellent). The printed dye **10** indicated very good-to-excellent results (4-5) while the printed dyes **8(a–d)** showed good-to-excellent results rating (2-5) against high temperature and staining as presented in Table 4. The good results of sublimation fastness contributed to the polarity of the substituent groups such as presence of OH and NH groups in dyes **10** and **8 (a–d)** [52].

Antibacterial activity

The target azo-disperse dye-printed samples were tested for their *in vitro* antibacterial activity against Gram-positive (, *i.e., Bacillus subtilis, Staphylococcus aureus,* and *Streptococcus faecalis*), and Gram-negative (*i.e., Pseudomonas aeruginosa, Escherichia coli,* and *Neisseria gonorrhoeae*) bacteria using the diffusion method [53]. The azo-disperse dye-printed samples activity increased by increasing the size of the zone of inhibition comparing to the reference drug Ampicillin as shown in Table 5. If the detected zone of inhibition is greater than or equal to the size of the reference drug inhibition zone, azo-disperse dye-printed samples are sensitive. Our investigation showed that the untreated polyester fabrics had no antibacterial activities against selected pathogenic bacteria. On the other hand, the starting materials (**1** and **3**) exhibit low antibacterial activities with inhibition zones ranging between 9 and 10 mm. Among all tested samples, polyester loaded with azo dye **8 a** was found to be highly active against all the tested bacterial strains followed by polyester loaded with **8 c**. Data analysis highlighted that polyester fabrics treated with azo dyes **8 (a–d)** showed broad spectrum than azo dye **10** of antibacterial activities with varied inhibition zones when compared to reference drug Ampicillin. The azo compound **8a** showed

Table 4 Sublimation fastness properties of the polyester fabric printed with dyes **8(a–d) and 10**

Sample	Sublimation fastness at 180 °C	Sublimation fastness at 210 °C	Staining on fabric after sublimation polyester	Staining on fabric after sublimation cotton
8 a	4–5	4–5	3–4	4
8 b	4	3–4	3–4	3–4
8 c	4	3–4	4	3–4
8 d	4–5	3–4	3–4	2–3
10	4–5	4–5	4–5	4–5

Table 5 Antibacterial activity for polyester-printed azo-disperse dyes against Gram-positive and Gram-negative bacteria after 4 washing cycles

Compounds		Diameter of inhibition zone (mm)					
		Gram-positive			Gram-negative		
		B. subtilis	*S. saureus*	*S. faecalis*	*E. coli*	*N. gonorrhoeae*	*P. aeruginosa*
Ampicillin		26	21	27	25	28	26
1		10	9	9	10	9	9
3a		–	–	9	–	–	–
3b		13	12	11	13	10	10
Untreated polyester		–	–	–	–	–	–
Polyester treated with	8a	19	23	17	18	17	15
	8b	13	10	11	12	11	11
	8c	13	16	14	14	13	13
	8d	12	10	12	11	12	10
		–	–	12	–	–	–

the best antibacterial activity against *S. aureus* with inhibition zone of 23 mm which is higher than the reference drug Ampicillin with inhibition zone 21 mm. Table 5 illustrates results of the polyester fabrics dyed with synthesized dyes after washing four times. The inhibitory effect of the newly synthesized azo dyes could be attributed to their efficacy to adhering to the bacterial cell wall and cytoplasmic membrane and then changing in selective permeability function which leads to the leakage of the cellular components and hence bacterial death [54]. Also, the synthesis of new azo-cleaved compound such as amines as a result of entering azo dyes to bacterial cells are responsible for toxic effects [55, 56]. Moreover, the newly synthesized compounds can be inhibited bacterial growth through inactivation of protein synthesis via reacting with thiol group [57], or inhibit DNA replication through reacting with phosphorus moieties [58].

Conclusion

New class of azo dyes containing quinoline chromophore was designed, synthesized, and characterized. The synthesized dyes were applied for silkscreen printing on polyester fabrics. Color measurements and fastness properties of the prepared dyes exhibited a high efficiency for washing, perspiration, rubbing, light, and sublimation fastness. The satisfactory performance and good antibacterial properties of the synthesized dyes lead to design of novel antibacterial disperse dyes with increasing the efficacy of application properties.

Acknowledgements The authors are grateful to the Electrochemistry Research Laboratory, Faculty of Electronic Engineering, Menoufia University, Egypt, for providing all facilities of research work.

Declarations

Conflict of interest No conflicts of interest.

References

1. K.D. Thomas, A. Adhikari, N. Shetty, Eur. J. Med. Chem. **45**, 3803–3810 (2010)
2. D. Verbanac, R. Malik, M. Chand, K. Kushwaha, M. Vashist, M. Matijašić, V. Stepanić, M. Perić, H.Č Paljetak, L. Saso, J. Enzyme Inhib. Med. **31**, 104–110 (2016)
3. J. Geng, D. Xu, X.-L. Zhao, Y.-N. Feng, H.-F. Qian, Y. Dai, W. Huang, RSC Adv. **6**, 101115–101122 (2016)
4. Z.-H. Cui, G. Xia, J.-R. Gao, W.-G. Chen, N.-P. Liu, Q. Ou, R.-L. Wang, Fibers Polym. **18**, 1708–1717 (2017)
5. S. Benkhaya, S. M'Rabet, A. El Harfi, Heliyon. **6**, e03271 (2020)
6. X.-Y. Jin, H. Chen, D.-D. Li, A.L. Li, W.-Y. Wang, W. Gu, J. Enzyme Inhib. Med. **34**, 955–972 (2019)
7. V.R. Solomon, S. Pundir, H. Lee, Sci. Rep. **9**, 6315 (2019)
8. A. Aboelnaga, T.H. El-Sayed, Green Chem. Lett. Rev. **11**, 254–263 (2018)
9. H.L. Yadav, P. Gupta, R.S. Pawar, P.K. Singour, U.K. Patil, Med. Chem. Res. **20**, 461–465 (2011)
10. V.M. Dembitsky, T.A. Gloriozova, V.V. Poroikov, Nat. Prod. Bioprospect. **7**, 151–169 (2017)
11. H. Shaki, Fibers Polym. **21**, 2530–2538 (2020)
12. M.E. Guerra, M. Llompart, C. Garcia-Jares, Cosmetics **5**, 47 (2018)
13. I. Minoru, T. Ohzono, T. Yamaguchi, Y. Norikane, Sci. Rep. **7**, 1–6 (2017)
14. J. Choi, W. Lee, J.W. Namgoong, T.-M. Kim, J.P. Kim, Dyes Pigm. **99**, 357–365 (2013)
15. F. Mohamed, M. Bashandy, H. Abd El-Wahab, M. Basseem, M. El-Molla, A. Bedair, J. Adv. Res. **2**, 248–260 (2014)
16. H. Shaki, K. Gharanjig, S. Rouhani, A. Khosravi, J. Fakhar, Color. Technol. **128**, 270–275 (2012)
17. A. Gurses, M. Açıkyıldız, K. Güneş, and M. Gürses, Dyes and Pigments: Their Structure and Properties. pp. 13–29 (2016)
18. R. Gup, E. Giziroglu, B. Kırkan, Dyes Pigm. **73**, 40–46 (2007)
19. A. Ceylan, S. Baş, M. Bayrakcı, S. Ertul, A. Uysal, Acta Chim. Slov. **59**, 656–663 (2012)
20. R. Dixit, A. Bulsara, H. Mehta, B. Dixit, J. Saudi Chem. Soc. **16**, 193–197 (2012)
21. A.Z. El-Sonbati, M.I. Abou-Dobara, M.A. Diab, A.A. El-Bindary, S.G. Nozha, Res. Chem. Intermed. **42**, 6449–6481 (2016)
22. D. Akram, I.A. Elhaty, and S.S. AlNeyadi. **8** (2020)
23. R.L.M. Allen, The chemistry of azo dyes, in *Colour Chemistry*. ed. by R.L.M. Allen (Springer, Boston, 1971), pp. 21–36
24. A. Kumar, K. Srivastava, S. Kumar, M. Siddiqi, S.K. Puri, J. Sexana, P.M.S. Chauhan, Eur. J. Med. Chem. **46**, 676–690 (2011)
25. I.E. Sayed, Am. J. Sci. **7**, 181–189 (2011)
26. M. Sharma, K. Chauhan, S. Chauhan, A. Kumar, S. Singh, J. Saxena, P. Agarwal, K. Srivastava, S. Kumar, S.K. Puri, Med. Chem. Commun. **3**, 71–79 (2012)
27. M. Molnar, B. Harshad, V. Rastija, V. Pavić, M. Komar, M. Karnaš, J. Babic, Molecules (Basel Switzerland) **23**, 1897 (2018)
28. D. Novaković, N. Kašiković, G. Vladić, M. Pál, 15 - Screen Printing, in *Printing on Polymers*. ed. by J. Izdebska, S. Thomas (William Andrew Publishing, Norwich, 2016), pp. 247–261
29. A. Mohmed, A. Fouda, M. Abdel-Rahman, S. Hassan, S. Gamal, S. Salah Salem, T.I. Shaheen, Biocatal. Agric. Biotechnol. **19**, 101103 (2019)
30. W.J. Brown, Antimicrob Agents Chemother. **32**, 385–390 (1988)
31. M.A. Pfaller, L. Burmeister, M.S. Bartlett, M.G. Rinaldi, J. Clin. Microbiol. **26**, 1437–1441 (1988)
32. J.A. Kiehlbauch, G.E. Hannett, M. Salfinger, W. Archinal, C. Monserrat, C. Carlyn, J. Clin. Microbiol. **38**, 3341–3348 (2000)
33. D. Fresco, M. Coles, R.G. Heimberg, M. Liebowitz, S. Hami, M.B. Stein, D. Goetz, Psychol. Med. **31**, 1025–1035 (2001)
34. N. Chadha, O. Silakari, Chapter 5—Thiazolidine-2,4-Dione: A Potential Weapon for Targeting Multiple Pathological Conditions, in *Key Heterocycle Cores for Designing Multitargeting Molecules*. ed. by O. Silakari (Elsevier, Amsterdam, 2018), pp. 175–209
35. K. van Beurden, S. de Koning, D. Molendijk, J. van Schijndel, Green Chem. Lett. Rev. **13**, 349–364 (2020)
36. A.U. Salami, Y.M. Kabir, B.K. Ademola, N.P. Obinna, H.A. Ziyaei, J. Serbian Chem. Soc. **85**, 1253–1264 (2020)
37. J.M. Jabar, A.I. Ogunmokun, T.A.A. Taleat, Fash. Text. **7**, 1 (2020)
38. N. Ahmed, S. Nassar, F. Kantouch, R.M. El-Shishtawy, Egypt. J. Chem. **63**, 1–14 (2020)
39. M.R. Luo, CIELAB, in *Encyclopedia of Color Science and Technology*. ed. by R. Luo (Springer, Berlin, Heidelberg, 2014), pp. 1–7

40. Textiles: Tests for colour fastness. Part C06: Colour fastness to domestic and commercial laundering. p. 9 (2010)
41. Textiles: Tests for colour fastness. Part X12: Colour fastness to rubbing. p. 5 (2016)
42. Textiles: Tests for colour fastness. Part E04: Colour fastness to perspiration. p. 5 (2013)
43. Textiles: Tests for colour fastness. Part P01: Colour fastness to dry heat (excluding pressing). p. 3 (1993)
44. Textiles: Tests for colour fastness. Part B02: Colour fastness to artificial light: Xenon arc fading lamp test. p. 35 (2013)
45. M. Sadeghi-Kiakhani, S. Safapour, Color. Technol. **131**, 142–148 (2015)
46. S.M. Al-Mousawi, M.A. El-Apasery, Molecules (Basel, Switzerland) **18**, 8837–8844 (2013)
47. M.M. Rahman, T.M.A. Haque, N.S. Sourav, S. Rahman, S. Yesmin, R. Mia, A. Al Noman, K. Begum, J. Iran. Chem. Soc. **18**, 817–826 (2021)
48. Y. Mahmoud Elkholy, M. Helmy Helal, A. Wahba Erian, Pigm. Resin. Technol. **30**, 168–171 (2001)
49. D.M. Patel, T.S. Patel, B.C. Dixit, J. Saudi Chem. Soc. **17**, 203–209 (2013)
50. A. Ketema, A. Worku, J. Chem. **2020**, 7 (2020)
51. A.M. Al-Etaibi, M.A. El-Apasery, Int. J. Environ. Res. Public Health **17**, 4714 (2020)
52. J.O. Otutu, E.M. Efurhievwe, S.U. Ameru, Chem. Mater. **6**, 40–46 (2014)
53. M. Balouiri, M. Sadiki, S.K. Ibnsouda, J. Pharm. Anal. **6**, 71–79 (2016)
54. S.S. Salem, A. Mohamed, M. El-Gamal, M. Talat, A. Fouda, EJCHEM. **62**, 1799–1813 (2019)
55. T. Deb, D. Ganguly, S. Sen, P. Giri, P. Dhar, S. Das, J. Chem. Sci. **130**, 94 (2018)
56. A.M. Soliman, W. Abdel-Latif, I.H. Shehata, A. Fouda, A.M. Abdo, Y.M. Ahmed, Biol. Trace Elem. Res. **199**, 800–811 (2020)
57. S. Alsharif, S. Salah Salem, M. Abdel-Rahman, A. Fouda, A. Eid, E.-D. Saad, S. Hassan, M. Ahmed Awad, A. Mohamed, Heliyon **6**, 03943 (2020)
58. A. Fouda, G. Abdel-Maksoud, M.A. Abdel-Rahman, A.M. Eid, M.G. Barghoth, M.A.-H. El-Sadany, Cellulose **26**, 6583–6597 (2019)